Photographing Impact of Plasma-Sprayed Particles on Metal Substrates

McDonald, A.; Chandra, S.; Lamontagne, M.; Moreau, C.

Publisher's version / Version de l'éditeur:

Proceedings of the International Thermal Spray Conference 2006, 2006-05-15

NRC Publications Record / Notice d'Archives des publications de CNRC:
https://nrc-publications.canada.ca/eng/view/object/?id=520333fd-87c9-47a9-afcc-8a7ac40001c9
https://publications-cnrc.canada.ca/fra/voir/objet/?id=520333fd-87c9-47a9-afcc-8a7ac40001c9

Photographing Impact of Plasma-Sprayed Particles on Metal Substrates

A. McDonald and S. Chandra
Department of Mechanical Engineering, University of Toronto, Toronto, Ontario, Canada

M. Lamontagne and C. Moreau
Industrial Materials Institute, National Research Council Canada, Boucherville, Québec, Canada

Abstract

Plasma-sprayed, molten molybdenum particles (~40 μm diameter) were photographed during impact (with velocity ~110 m/s) on inconel surfaces that were preheated or maintained at room temperature or 400°C. A droplet approaching the surface was sensed using a photodetector and after a known delay, a fast CCD camera was triggered to capture images of the spreading splat from the substrate front surface. A rapid two-color pyrometer was used to collect the thermal radiation from the impacting particles to follow the evolution of their temperature and size after impact. Molten molybdenum particles impacting on the surfaces at room temperature disintegrated and splashed, after achieving a maximum diameter larger than 400 μm. Impact on preheated and heated inconel produced splats with maximum diameters between 200 μm and 300 μm and with less splashing. The cooling rate of splats on the preheated inconel was larger than that of splats on non-heated inconel, suggesting that the splat-substrate contact was improved.

Introduction

Studies have shown that the temperature and surface conditions of the substrate on which plasma-sprayed particles impact influences the extent of splashing and splat morphology [1 - 5]. Fukumoto, *et al.* [2] and Moreau, *et al.* [4] have shown that increasing the substrate temperature reduced the occurrence of splashing and produced disk-like splats. Fukumoto, *et al.* [2] speculated that the disk-like splats were formed due to good contact between the substrate and splat, increasing the solidification rate of the splat. Moreau, *et al.* [4] and McDonald, *et al.* [6] showed that the cooling rate of molybdenum splats on heated glass was an order magnitude larger than that on non-heated glass.

The surface condition of the substrates have been shown to have an impact on the spreading dynamics of the splat. Jiang, *et al.* [7] have shown that removal of condensates and adsorbates from a cold stainless steel substrate will eliminate splashing and splat fragmentation of impacting molten ZrO_2 and produce contiguous, disk-like splats. The formation of the disk-like splats were attributed to improved contact between the splat and substrate, in the absence of the condensates and adsorbates. It was also shown that the same contiguous, disk-like morphology occurred for splats on a substrate held at 500°C. Cedelle, *et al.* [8] and Fukumoto, *et al.* [9] have shown that preheating a metal substrate for several hours also changes the surface due to the formation of an oxide layer. It was proposed that this oxide layer increases the wettability of the splat on the substrate, reducing splashing and producing disk-like splats.

Photographs and two-color pyrometry have been used to obtain the splat size, temperature evolution, and the cooling rate. Cedelle, *et al.* [10] used the temperature evolution obtained from two-color pyrometry to show that the cooling rate of nickel on a preheated stainless steel substrate is almost an order of magnitude larger than that on non-heated stainless steel. Photographs captured with a fast CCD camera show that the splats had a disk-like morphology.

The objectives of this study were to: (1) to photograph molybdenum particles that impacted preheated inconel and inconel maintained at room temperature and at 400°C; (2) use two-color pyrometry to measure the temperature evolution and cooling rates of the splats on these surfaces; and (3) compare the results on inconel with those on glass exposed to the same conditions.

Experimental Method

A schematic diagram of the experimental setup is shown in Figure 1. A SG100 torch (Praxair Surface Technologies, Indianapolis, IN) was used to melt and accelerate molybdenum (SD152, Osram Sylvania Chemical and Metallurgical Products, Towanda, PA) powder particles, seived to +38 -60 μm. The powder feed rate was less than 1 g/min. The substrates were mirror-polished inconel and glass slides (Fisher Scientific, Pittsburgh, PA) that were washed

with water and ethanol and dried in an oven at 140°C for 30 minutes. The back of the glass slides were painted black to provide a contrasting background when splat images were captured. In order to heat the substrate during spraying, the samples were placed in a copper substrate holder that included resistance heater wires. Some inconel and glass samples were heat-treated in air for 3 hours at 400°C and allowed to cool.

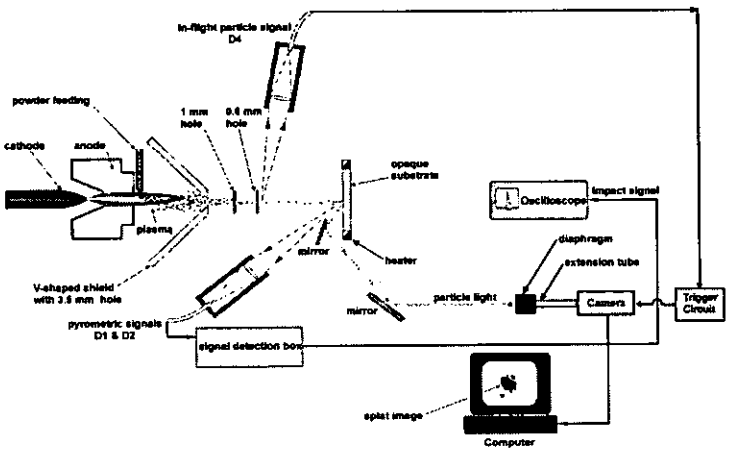

Figure 1: Schematic of the experimental assembly

The plasma torch was operated with a voltage of 35 V and a current of 700 A. The carrier gas mixture was argon at a flow rate of 50 liters per minute (LPM) and helium at 24.5 LPM. The torch was passed rapidly across the substrates. In order to protect the substrate from an excess of particles and heat, a V-shaped barrier was placed in front of the torch. This V-shaped shield had a 3.5 mm hole through which particles could pass. To reduce the number of particles landing on the substrate, two additional barriers were placed in front of the substrate, the first of which had a 1 mm hole and the second, a 0.6 mm hole. All the holes were aligned to permit passage of the particles with a horizontal trajectory.

After exiting the third barrier and just before impacting the substrate, the thermal radiation of the particles was measured with a 2-color pyrometric system. This system included an optical sensor head that consisted of a custom-made lens, which focused the collected radiation, with a 0.21 magnification, on an optical fiber with an 800 μm core [5]. This optical fiber was covered with an optical mask that was opaque to near infrared radiation, except for three slits (see Fig. 2a). The two smaller slits, with dimensions of 30 μm by 150 μm and 30 μm by 300 μm, were used to detect the thermal radiation of the particles in flight. The radiation was used to calculate the temperature, velocity, and diameter of the in-flight particles [5,11]. The largest slit, measuring 150 μm by 300 μm, was used to collect thermal radiation of the particle as it impacted and spread on the substrate. With the thermal radiation from this slit, the splat temperature, diameter, and cooling rate were calculated at 200 ns intervals after impact.

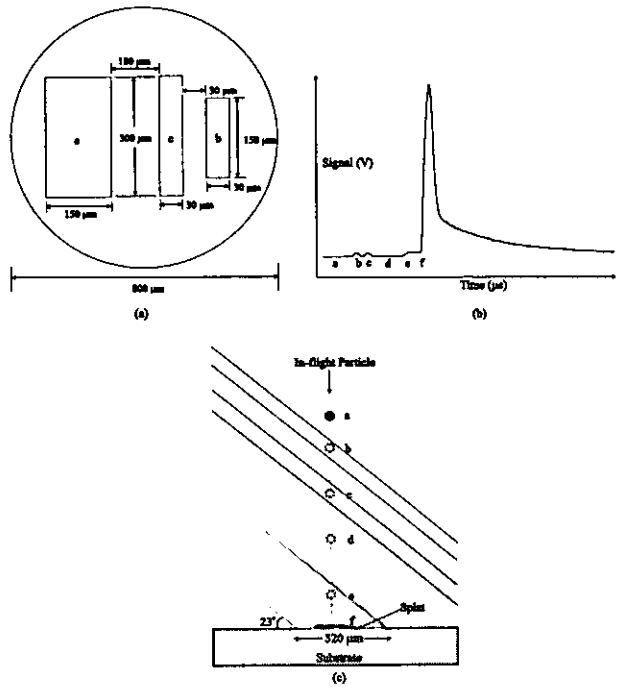

Figure 2: a) Details of the 3-slit mask, b) A typical signal collected by the 3-slit mask, c) Schematic of the optical detector fields of view

The collected thermal radiation was transmitted through the optical fiber to a detection unit that contained optical filters and two photodetectors. The radiation beam was divided into two equal parts by a beam splitter. Each signal was transmitted through a bandpass filter with wavelength of either 785 nm or 995 nm in order to segregate the radiation into two parts. The ratio of the radiation intensity at these wavelengths (referred to as D_1 and D_2, respectively) was used to calculate the particle temperatures with an accuracy of ± 100°C [11]. The signals were recorded and stored by a digital oscilloscope.

A typical signal captured by the system is shown in figure 2b. The labels, *a-f*, correspond to the position of a particle (shown in Fig. 2c) as it passes through the field of views of each of the optical slits. At points *a* and *d*, the particle was not in an optical field of view, so the signal voltage was zero. The two peaks at points *b* and *c* were produced by thermal emissions from the particle as it passed through the first two small slits. The droplet average in-flight velocity was calculated by dividing the known distance between the centers of the fields of view of the two slits by the measured time of flight. At point *e* the droplet entered the field of view of the third and largest optical slit. This is shown on the thermal signal by a plateau in the profile. Upon impact at *f*, the signal increases as the particle spreads and eventually decreases as the particle cools down and/or splashes out of the field of view.

A 12-bit CCD camera (QImaging, Burnaby, BC) was used to capture images of the spreading particles. The electronic shutter of the camera was triggered to open by a signal from the D_4 sensor (Fig. 1). The camera was attached to a 12-inch long optical extension tube that was connected to a diaphragm (Tominon, Waltam, MA). The diaphragm included a lens with a 135-mm focal length and a numerical opening from 4.5 to 32. The diaphragm was set to a numerical opening of 16, so that the diameter was 8.4-mm. In order to photograph the particle in-flight and during spreading and capture integrated images, the shutter of the camera was opened for about 500 μs. The images captured by the camera were then digitized by a frame grabber and recorded on a personal computer.

Results and Discussion

Impact on inconel

Figures 3, 4, and 5 show typical thermal emission signals from the D_1 (785 nm) sensor, the temperature evolution, and integrated images of different particles on inconel held at 400°C, room temperature, and on samples heated to 400°C, then cooled (preheated), respectively. The thermal emission signals were used to calculate the in-flight temperature and velocity of the particle and the maximum spread time of the splat. The time of impact is indicated as t = 0 μs on the graphs. The maximum spread time is taken as the time required for reaching the maximum voltage on the thermal emission signals. This corresponds closely to the moment the splat reaches its maximum diameter. The average in-flight temperature of the particles was 2830 °C and the average in-flight velocity was 110 m/s. In addition to the splats at the maximum extent, the images also show two comet-like streaks. One streak represents the path of the particle in-flight and the other, its reflection in the mirror-polished inconel. The ImageJ imaging software (National Institute of Health, Washington D.C.) was used to estimate the maximum diameters from the images by calculating the area A_c and perimeter P of the circular, white splats and using the hydraulic diameter formula, $D_{\max} = \frac{4A_c}{P}$. The in-flight particle diameters were estimated by measuring the width of the comet-like streaks in the images.

On inconel heated to 400°C, the particles spread to an average maximum diameter of 165 μm in ~0.5 μs (Fig. 3). On inconel held at room temperature, the average maximum spread diameter was almost 3 times larger (440 μm). The maximum spread time was ~1.1 μs (Fig. 4). The morphology of the splats at the maximum extent on preheated inconel was similar to that on non-heated inconel. The maximum spread diameter on this substrate was 320 μm, with a maximum spread time of ~0.6 μs (Fig. 5). For the impact of 50 μm molybdenum particles on glass, McDonald, *et al.* [6] have shown that the maximum spread diameters on glass heated to 400°C was ~200 μm and on non-heated glass, it was ~500 μm. The maximum spread times were ~0.8 and ~ 1.9 μs, respectively. These results suggest that the type of substrate affects only slightly the maximum spread diameter and time.

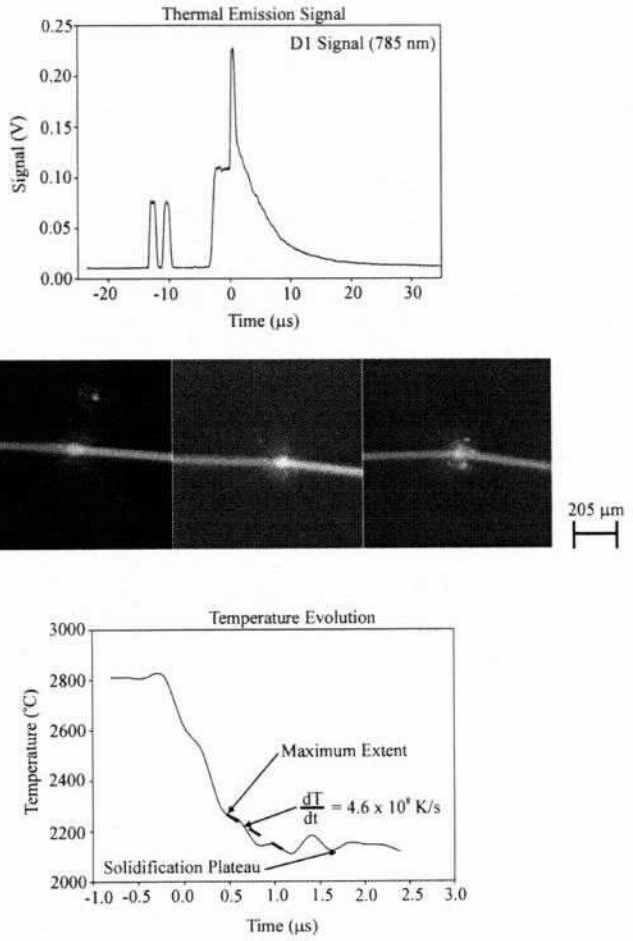

Figure 3: A typical thermal emission signal, the splat temperature evolution, and images of molybdenum splats on inconel held at 400°C.

Moreau, *et al.* [12] have shown that on a typical thermal emission signal for the impact of molybdenum on non-heated surfaces, the transition from a period of relatively high voltage decrease, immediately after achieving the maximum diameter, to a period of slow voltage decrease indicates that material splashes and exits the pyrometric field of view. The thermal emission signal of the splat that impacted the non-heated inconel (Fig. 4) shows this transition approximately 2 μs after impact. Figures 3 and 5, which show the impact on heated and preheated inconel, do not show this transition. The temperature evolution of the splats during spreading are also shown in the figures (Figs. 3, 4, 5). The cooling rate of the splat was calculated from the temperature at the maximum extent to either the solidification plateau, in the case of the splats on inconel held at 400°C or preheated, or to the point where splashing began on the non-heated surface, approximately 2 μs after impact. Several investigators [2 – 4,

6] have shown that the impact on heated surfaces result in significantly less splat fragmentation and splashing. The figures show that the cooling rate on inconel held at 400°C (4.6×10^8 K/s) is more than 4 times larger than that on non-heated inconel (1.2×10^8 K/s), but two times larger than on preheated inconel (2.3×10^8 K/s). The differences in the cooling rates suggest that the physical contact between the splat and the inconel held at 400°C is improved by heating, increasing the heat transfer. This has been attributed to the absence of adsorbates/condensates on the heated surface [7]. On heated glass, the cooling rate was 2.2×10^8 K/s and on non-heated glass, it was 4.7×10^7 K/s [6].

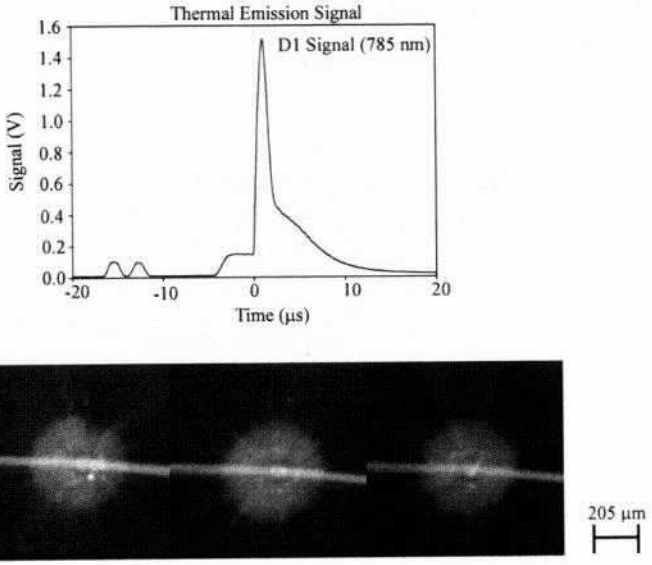

Figure 4: A typical thermal emission signal, the splat temperature evolution, and images of molybdenum splats on inconel held at room temperature.

McDonald, *et al.* [6] observed that when the cooling rate was on the order of 10^8 K/s (as on heated glass and inconel), the temperature of the liquid splat fell below the molybdenum melting point (2617 °C), a few microseconds after impact. Figures 3 - 5 show that on all inconel surfaces, the temperature of the liquid splat fell below the melting point, possibly due to undercooling [6].

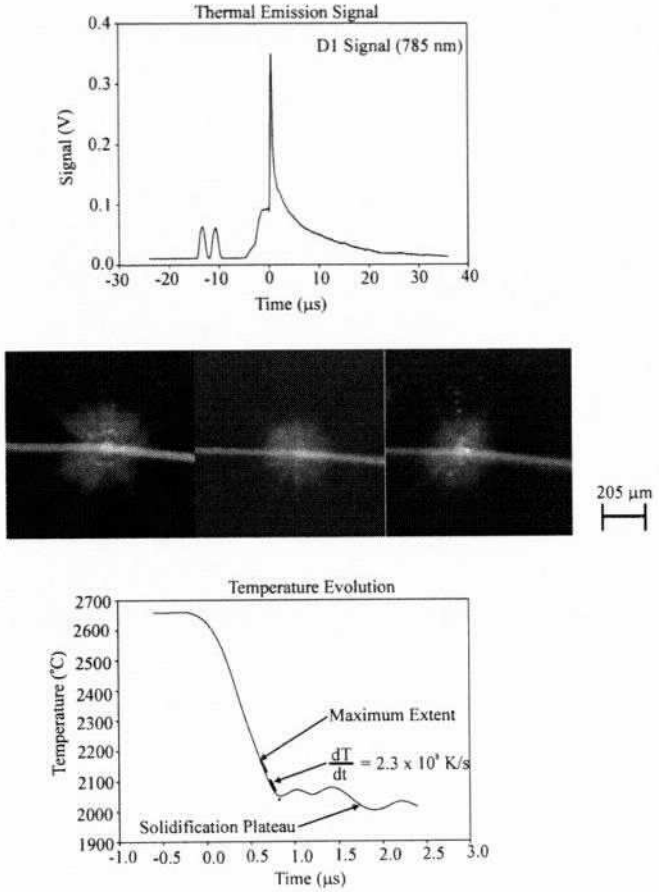

Figure 5: A typical thermal emission signal, the splat temperature evolution, and images of molybdenum splats on inconel heated to 400°C, then cooled.

Analysis of the inconel surface

Atomic force microscopy (AFM) was used to determine the roughness and profile of the substrate surface. Figure 6 shows images of the surfaces of non-heated and preheated inconel and the corresponding surface roughness. It is observed that the number of small projections on the preheated surface is larger than on the non-heated surface. Fukumoto, *et al.* [9] have shown similar images for preheated and non-heated AISI304 steel. They have also shown that the oxide layer on the preheated metal could be as much as ten times thicker. The average roughness (R_a) on the preheated inconel was 3.4 nm and on the non-heated inconel, it was 2.1 nm. Figure 7 shows that preheating glass changes the surface topology and roughness slightly, with the average roughness decreasing from 1.1 nm to 0.58 nm.

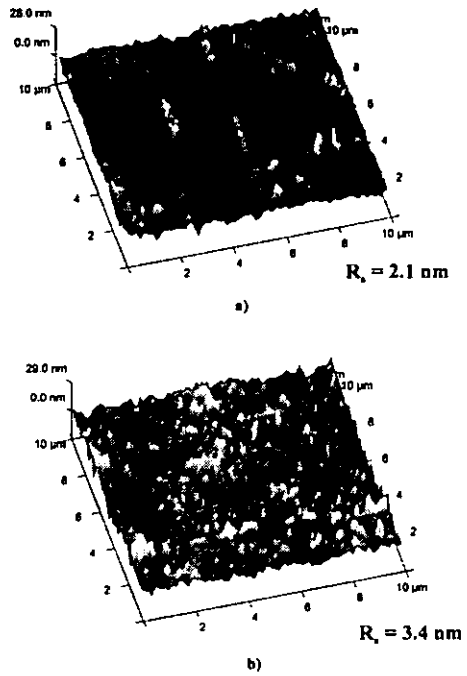

Figure 6: a) Surface topology of inconel a) held at room temperature and b) heated to 400°C, then cooled.

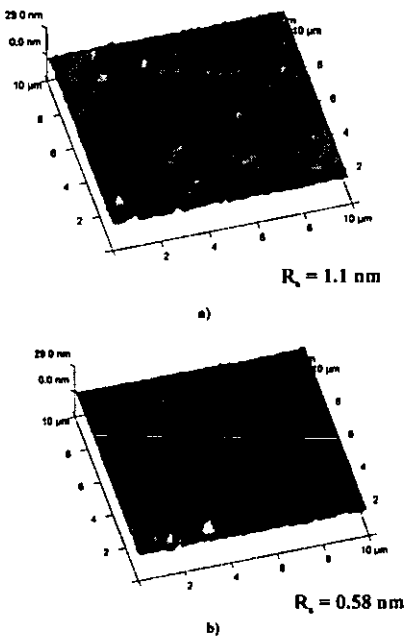

Figure 7: a) Surface topology of glass a) held at room temperature and b) heated to 400°C, then cooled.

Comparison of impact on inconel and glass

The D_I thermal emission signals and images of the splats on inconel and glass heated and maintained at 400°C and on preheated inconel are shown in figure 8. From the thermal emission signals and photos, the maximum spread diameter on the heated inconel and glass is approximately 200 μm. On the preheated inconel, the maximum spread diameter is larger (320 μm), so the maximum voltage on the thermal emission signal is larger (0.35 V). Figure 9 shows the D_I thermal emission signals and images of the splats on non-heated inconel and glass and on preheated glass. Preheating glass has little effect on the spreading of the molybdenum particle, compared to on non-heated glass. The maximum spread diameter, on both surfaces, is approximately 410 μm and the maximum spread time is about 1.8 μs.

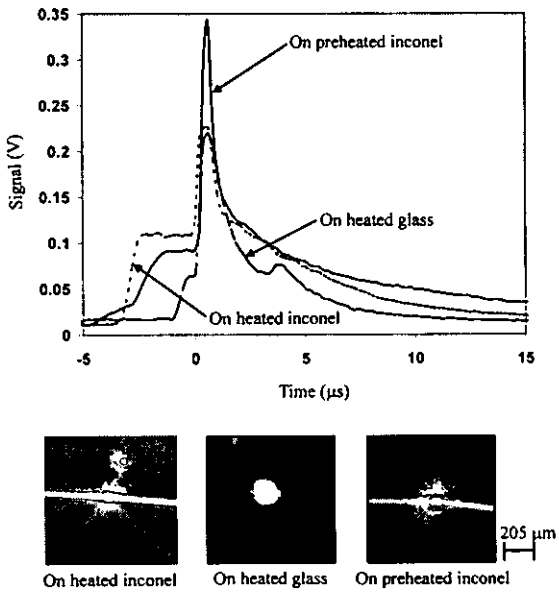

Figure 8: Comparison of the thermal emission signals of molybdenum that impacted preheated inconel and inconel and glass held at 400°C.

The images and thermal emission signals of figures 8 and 9 show that for splats on the inconel or glass substrates held at room temperature or at 400°C, the maximum spread diameters, the maximum spread time, and the point of splashing (Fig. 9) was not affected significantly by the substrate. In figure 8, the maximum thermal emission signal voltage is about 0.30 V and in figure 9, it is about 2.0 V for splats on both surfaces.

The larger cooling rate and maximum spread diameter on the preheated inconel, compared to splats on the non-heated inconel, indicate that the contact between the surface and splat is better, probably due to improved contact on the rougher, oxidized surface. On glass substrates, maintaining the substrate at 400°C evaporates condensates and adsorbates [7], without further oxidizing the surface. Impact on cold and preheated glass suggests that the contaminants are readsorbed onto the preheated surface during cooling, since the splat spread dynamics are similar on cold and preheated glass (Fig. 9).

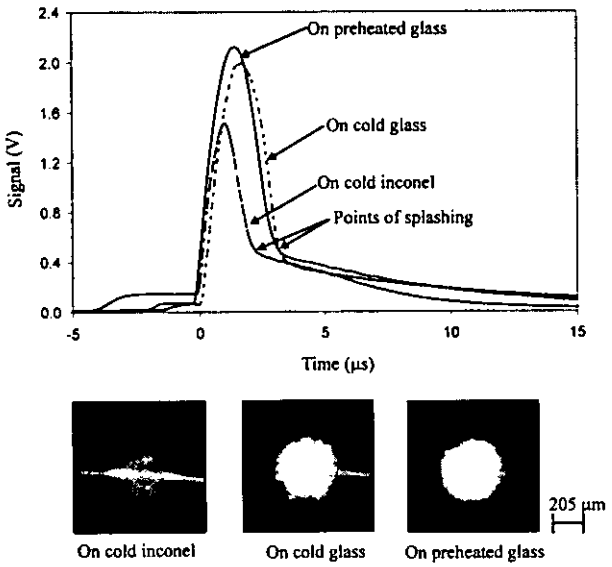

Figure 9: Comparison of the thermal emission signals of molybdenum that impacted preheated glass and inconel and glass held at room temperature (cold).

Conclusion

The influence of substrate temperature and surface conditions on the splat morphology, the maximum spread diameter, and the cooling rate of plasma-sprayed molybdenum particles was studied. Plasma-sprayed molybdenum particles that impacted inconel maintained at room temperature had a maximum spread diameter that was almost 3 times that on inconel maintained at 400°C. The cooling rate, as calculated from 2-color pyrometric signals, is more than 3 times larger on the heated inconel, suggesting that thermal contact was improved.

Comparison of the thermal emission signals and the splat indicate that the spreading dynamics on inconel and glass maintained at room temperature were similar. Similar results were also obtained for impact on inconel and glass maintained at 400°C.

Particles that impacted inconel that was heated for 3 hours at 400°C and then cooled showed reduced disintegration, compared to particles that impacted non-heated inconel. The splat maximum diameter was smaller on the preheated surface, while the cooling rate was more than 2 times larger than on non-heated inconel. Increased roughness and changes in the surface topography due to oxidation on preheated inconel suggested that contact between the splat and surface was improved, increasing the cooling rate, while decreasing the maximum spread diameter.

References

1. M. Pasandideh-Fard, V. Pershin, S. Chandra, and J. Mostaghimi, Splat shapes in a thermal spray coating process: Simulations and experiments, *J. of Thermal Spray Tech.*, Vol 11 (No. 2), 2002, p. 206 – 217
2. M. Fukumoto, E. Nishioka, and T. Matsubara, Flattening and solidification behavior of a metal droplet on a flat substrate surface held at various temperatures, *Surf. Coat. Tech.*, Vol 120 – 121, 1999, p. 131 – 137
3. M. Fukumoto, Y. Huang, and M. Ohwatari, Flattening mechanism in thermal sprayed particle impinging on flat substrate, *Thermal Spray: Meeting the Challenges of the 21st Century*, C. Coddet, Ed., May 25-29, 1998 (Nice, France), ASM International, 1998, p. 401 – 406
4. C. Moreau, J. Bisson, R. Lima, and B. Marple, Diagnostics for advanced materials processing by plasma spraying, *Pure Appl. Chemistry*, Vol 77 (No. 2), 2005, p. 443 – 462
5. N. Mehdizadeh, M. Lamontagne, C. Moreau, and S. Chandra, Photographing impact of molten molybdenum particles in a plasma spray, *J. Thermal Spray Tech.*, Vol 14, 2005, p. 354 - 361
6. A. McDonald, M. Lamontagne, C. Moreau, and S. Chandra, Visualization of impact of plasma-sprayed molybdenum particles on hot and cold glass substrates, *International Thermal Spray Conference 2005*, Plasma Spraying, E. Lugscheider, Ed., May 2-4, 2005 (Basel, Switzerland), ASM International, 2005, p. 1192 – 1197
7. X. Jiang, Y. Wan, H. Hermann, S. Sampath, Role of Condensates and Adsorbates on Substrate Surface on Fragmentation of Impinging Molten Droplets During Thermal Spray, *Thin Solid Films*, Vol 385, 2001, p. 132 – 141
8. J. Cedelle, M. Vardelle, P. Fauchais, and M. Fukumoto, Thermal behavior at impact of micrometre and millimetre sized particles, Influence of substrate roughness and skewness, *International Thermal Spray Conference 2005*, Plasma Spraying, E. Lugscheider, Ed., May 2-4, 2005 (Basel, Switzerland), ASM International, 2005, p. 1180 – 1186
9. M. Fukumoto, I. Ohgitani, M. Shiiba, and T. Yasui, Effect of substrate surface change by heating on transition in flattening behavior of thermal sprayed particles, *Thermal Spray 2004: Advances in Technology and Application*, Characterization Methods for Coating Properties (V), E. Lugscheider and C. Berndt, Eds., May 10-12, 2004 (Osaka, Japan), ASM International, 2004, p. 1 – 6
10. J. Cedelle, M. Vardelle, B. Pateyron, P. Fauchais, M. Fukumoto, and I. Ohgitani, Plasma-sprayed particles: Impact imaging and flattening particle thermal history, *International Thermal Spray Conference 2005*, Process Diagnostics (I), May 2-4, 2005 (Basel, Switzerland), ASM International, 2005, p. 656 – 661
11. C. Moreau, P. Cielo, M. Lamontagne, S. Dallaire, M. Vardelle, Impacting particle temperature monitoring during plasma spray deposition, *Meas. Sci. Technol.*, Vol 1, 1990, p. 807 – 814
12. C. Moreau, P. Gougeon, and M. Lamontagne, Influence of substrate preparation on the flattening and cooling of plasma-sprayed particles, *J. Thermal Spray Tech.*, Vol 4 (No. 1), 1995, p. 25 – 33